

# Cell Adhesion on Surface-Functionalized Magnesium

Victoria Wagener,<sup>†,§</sup> Achim Schilling,<sup>‡,§</sup> Astrid Mainka,<sup>‡</sup> Diana Hennig,<sup>†</sup> Richard Gerum,<sup>‡</sup> Marie-Luise Kelch,<sup>†</sup> Simon Keim,<sup>†</sup> Ben Fabry,<sup>‡,§</sup> and Sannakaisa Virtanen<sup>\*,†,§</sup>

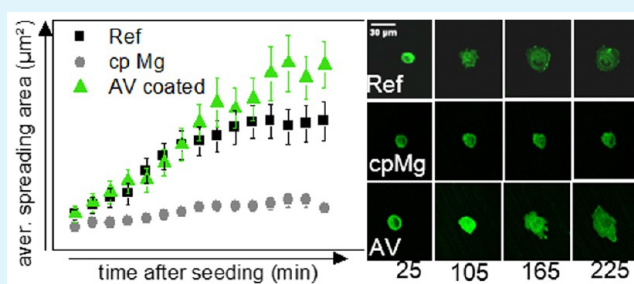
<sup>†</sup>Chair for Surface Science and Corrosion, Department of Materials Science, University Erlangen-Nuremberg, Martensstrasse 7, 91058 Erlangen, Germany

<sup>‡</sup>Biophysics Group, Department of Physics, University of Erlangen-Nuremberg, Henkestrasse 91, 91052 Erlangen, Germany

## Supporting Information

**ABSTRACT:** The biocompatibility of commercially pure magnesium-based (cp Mg) biodegradable implants is compromised of strong hydrogen evolution and surface alkalization due to high initial corrosion rates of cp Mg in the physiological environment. To mitigate this problem, the addition of corrosion-retarding alloying elements or coating of implant surfaces has been suggested. In the following work, we explored the effect of organic coatings on long-term cell growth. cp Mg was coated with aminopropyltriethoxysilane + vitamin C (AV), carbonyldiimidazole (CDI), or stearic acid (SA). All three coatings have been previously suggested to reduce initial corrosion and to enhance protein adsorption and hence cell adhesion on magnesium surfaces. Endothelial cells (DH1+/+) and osteosarcoma cells (MG63) were cultured on coated samples for up to 20 days. To quantify Mg corrosion, electrochemical impedance spectroscopy (EIS) was measured after 1, 3, and 5 days of cell culture. We also investigated the speed of initial cell spreading after seeding using fluorescently labeled fibroblasts (NIH/3T3). Hydrogen evolution after contact with cell culture medium was markedly decreased on AV- and SA-coated Mg compared to uncoated Mg. These coatings also showed improved cell adhesion and spreading after 24 h of culture comparable to tissue-treated plastic surfaces. On AV-coated cp Mg, a confluent layer of endothelial cells formed after 5 days and remained intact for up to 20 days. Together, these data demonstrate that surface coating with AV is a viable strategy for improving long-term biocompatibility of cp Mg-based implants. EIS measurements confirmed that the presence of a confluent cell layer increased the corrosion resistance.

**KEYWORDS:** cell adhesion, magnesium, organic coating, corrosion protection, impedance spectroscopy



## 1. INTRODUCTION

The strong initial corrosion of commercially pure magnesium (cp Mg) in physiological environments still remains a problem for its application as a biodegradable implant material.<sup>1–5</sup> Hydrogen evolution on the Mg surface may not only lead to gas cavitation but may also reduce or impede initial cell adhesion on the implant.<sup>5–8</sup> In addition, Mg dissolution induces an alkalization (pH increase) near the implant surface and may prevent cell attachment and growth.<sup>9</sup> Thus, cp Mg is thought to possess only limited initial biocompatibility due to its high initial corrosion rate in physiological environments.

For the successful use of Mg in biomedical devices, good cell adhesion on the implant surface is thought to be important. Thus, cell adhesion and proliferation is customarily taken as a measure for biocompatibility. In addition, a surface coverage with cells has been speculated to reduce Mg corrosion.<sup>9</sup>

Cell adhesion in a physiological environment consisting of a complex mixture of different proteins and peptides is unlikely to occur directly on the implant surface but rather is influenced by prior protein adsorption.<sup>10,11</sup> In addition to increasing corrosion resistance, therefore, it is hoped that an appropriate surface treatment of cp Mg may further enhance protein

adsorption and thus improve cell adhesion and biocompatibility.

In this work, cp Mg was coated with three different linker molecules that are known to immobilize proteins on the surface and have been used and analyzed previously by our group.<sup>12</sup> We then incubated the surface-functionalized samples in Dulbecco's modified Eagle's medium (DMEM) and measured hydrogen evolution over the course of 24 h. Furthermore, we measured the confluency and density of mouse endothelial (DH1+/+) and human osteosarcoma (MG63) cells after 24 h of incubation on differently functionalized cp Mg samples. These cell types were chosen based on possible application of Mg implants—cardiovascular stents and bone fixation. The time course of cell spreading during the first 5 h after seeding on functionalized cp Mg was measured using fluorescently labeled fibroblasts (GSP NIH3T3). Long-term cell tests of up to 20 days were performed on AV-coated cp Mg, which showed the best cell properties during short-term (24 h) tests.

**Received:** February 10, 2016

**Accepted:** April 18, 2016

**Published:** April 18, 2016

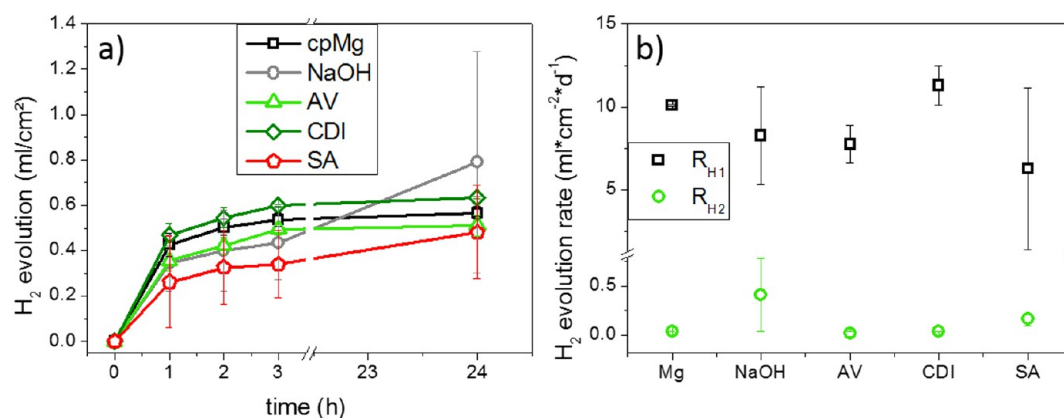


**Figure 1.** Hydrogen evolution measurements of cp Mg, NaOH-passivated Mg and after coating with AV, CDI, and SA: (a) hydrogen evolution vs time, mean  $\pm$  sd ( $n = 3$ ); (b) hydrogen evolution rates in the first hour of immersion ( $R_{H1}$ , black squares) and between 3 and 24 h ( $R_{H2}$ , blue circles) (mean  $\pm$  sd).

Electrochemical impedance spectroscopy confirmed earlier speculations that a cell layer can slow down Mg corrosion.

## 2. MATERIALS AND METHODS

**2.1. Sample Preparation.** For all experiments, cp Mg (99.9%) (Chempur, Karlsruhe, Germany) was used. The samples were cut from a Mg rod with a diameter of 9.5 or 25.4 mm as discs with an average thickness of 2–4 mm. After deburring, the samples were ground with a 1200 grit abrasive SiC disc and sonicated in ethanol.

**2.2. Passivation in 1 M NaOH.** For achieving a dense and homogeneous magnesium hydroxide (Mg(OH)<sub>2</sub>) layer, ground samples were passivated by boiling in 1 M sodium hydroxide (NaOH) for 20 min. Afterward, the samples were coated with the different molecules.

**2.3. Linker Molecule Coatings.** Aminopropyltriethoxysilane (APTES) plus ascorbic acid (vitamin C) (AV), carbonyldiimidazole (CDI), and stearic acid (SA) were used as linker molecules. Coating procedures were performed according to previous works.<sup>12–17</sup> In brief, for AV coating, the NaOH-passivated samples were immersed in 10 mM APTES solution in toluene (Aldrich, 99.8% purity) for 24 h at 70 °C, rinsed with acetone and ethanol, and sonicated in ethanol for 10 min.<sup>13,14</sup> Following Tiller et al.,<sup>15</sup> the APTES-modified substrates were immersed in a saturated solution of ascorbic acid (Sigma-Aldrich, puriss.) in dimethyl sulfoxide (DMSO; Aldrich, purity > 99.9%) for 30 min under gentle stirring. After rinsing with water, the samples were air-dried for at least 2.5 h to ensure the oxidation of the ascorbic acid molecules to dehydro-ascorbic acid. Proteins can bind unspecifically to the surface via reaction of a primary amino group to one of the keto groups of the dehydro-ascorbic acid, forming a peptide bond.<sup>18</sup>

For coating with CDI, the NaOH-passivated samples were immersed in a 25 mM solution of CDI (Sigma-Aldrich, reagent grade) in chloroform (Sigma-Aldrich, purity > 99.8%) for 6 h at room temperature and rinsed in chloroform for about 5 min.<sup>16</sup> The coupling of proteins is via primary amino groups as a substitution reaction.<sup>19</sup>

For coating with stearic acid (SA), we followed the procedure described by Wang et al.<sup>17</sup> The samples were immersed and stirred in 0.05 M SA (Sigma-Aldrich, reagent grade) solution in ethanol for 1 h at room temperature and rinsed in ethanol for 10 min. Proteins bind by hydrophobic interactions between the tail of the SA molecule and hydrophobic areas of the proteins.<sup>20,21</sup>

**2.4. Passivation in Cell Culture Medium.** For the passivation in cell culture medium, DMEM (41966; 1X, L-glutamine, pyruvate; Gibco by Life Technologies) with 20% FCS (fetal calf serum, Gibco), and 1% PSG (penicillin–streptomycin–L-glutamine 200 mM (100X), Gibco) were used. Ground (but not NaOH-passivated) Mg samples were immersed in 12 mL of cell culture medium at 37 °C in a cell culture incubator with 5% CO<sub>2</sub> and 95% humidity for 3 days.

**2.5. Cell Culture and Seeding.** For short- and long-term cell growth experiments, mouse endothelial cells (DH1+/+; gift from Gerhard Wiche) and human osteosarcoma cells (MG63; gift from Rainer Detsch) were used. For cell spreading experiments, fluorescent mouse NIH3T3 fibroblasts permanently transfected with actin-eGFP were chosen. Cells were cultured in T75 cell culture flasks in 10 mL of DMEM (41966; 1X, L-glutamine, pyruvate; Gibco), with a glucose concentration of 1 g/L for MG63 and DH1+/+ cells or 4.5 g/L for NIH3T3 cells, with 10% FCS (Sigma-Aldrich) for Mg63 and NIH3T3 cells, or 20% FCS for DH1+/+ cells; and with 1% PSG (200 mM (100X), 1:1:1; Gibco). A 1  $\mu$ g/mL amount of puromycin (Gibco) was added to the NIH3T3 medium as a selection agent. Cells were harvested with 0.25% trypsin–EDTA (Gibco) in PBS. Trypsin was neutralized with 20% FCS after a few seconds for the MG63 and NIH3T3 cells and after 1 min for the DH1+/+ cells.

For the cell tests on differently treated Mg, 50,000 cells were seeded on each sample. As reference, tissue culture plastic was used. For corrosion experiments—where sample surfaces were about four times larger—200,000 cells per sample were seeded. Cells were cultured on the different samples for 1, 5, 10, 15, and 20 days in the case of cell viability experiments and 1 and 5 days in the case of corrosion experiments. Cell culture medium was changed every second day in the beginning and each day after cultivation times longer than 5 days.

**2.6. Cell Fixation and Staining.** To determine cell number and density on Mg substrates after defined times, cells were fixed in 4% paraformaldehyde (Thermo Scientific) with 5  $\mu$ L/ml Triton X-100 (Sigma-Aldrich) in DPBS with 20% FCS for 20 min, followed by a washing step in DPBS with 10% FCS for a few minutes (note that the presence of FCS during fixation and staining is important to keep the Mg samples passivated; DPBS without FCS accelerates corrosion, and the resulting H<sub>2</sub> evolution diminishes the staining quality). Subsequently, cell nuclei were stained with 1.0  $\mu$ L/ml Sytox green (Life Technologies), and actin filaments were stained with 6.0  $\mu$ L/ml Phalloidin red (Sigma-Aldrich). The dyes were diluted in DPBS with 10% FCS. After staining for 60 min using 100  $\mu$ L of staining solution for d. 25.4 mm discs or 50  $\mu$ L for d. 10.0 mm discs, the samples were washed three times for 5 min in DPBS with 10% FCS, deionized water (a few seconds), isopropanol (90%, 96%, and 100%; each step for 5 min), and xylene (5 min) and finally fixed on a glass coverslip (Carl Roth) with water-free Eukit mounting medium (Fluka Analytical).

**2.7. Analysis of Cell Morphology, Proliferation, and Spreading.** Ten epifluorescence images (Leica DMI6000 B, Leica Microsystems) per sample were taken in stacks of four images with a z-distance of 2  $\mu$ m in order to account for the corroded surface which often made it impossible to obtain a focused single image of all the structures. Image evaluation was done in MATLAB. After maximum projection of the image stack, cells were counted using a segmentation algorithm based on Otsu's thresholding. The spreading area

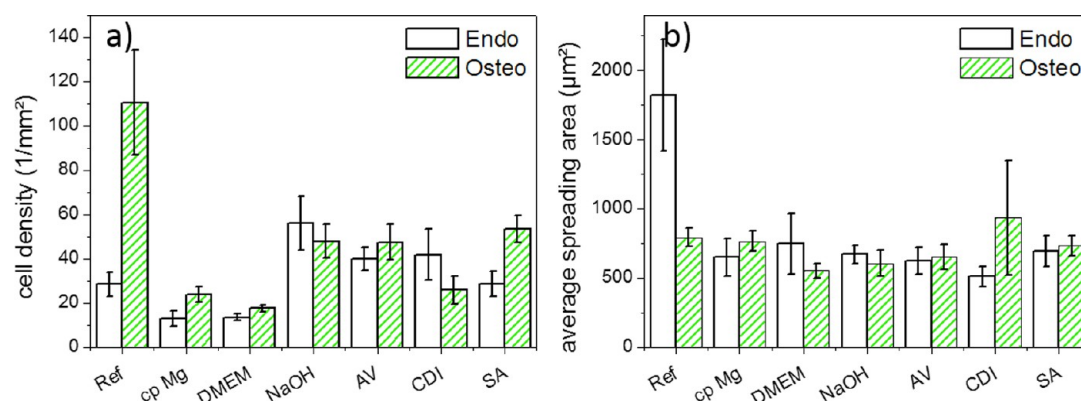


**Figure 2.** Cell density (a) and average spreading area (b) for the growth of endothelial and osteosarcoma cells for 1 day on Mg, after DMEM and NaOH passivation and after coating with the linker molecules AV, CDI, and SA (mean  $\pm$  se with  $n = 10$ ). As reference, tissue culture plastic with the same dimensions was used.

calculation was performed with the “canny” edge detection algorithm after contrast spreading.

**2.8. In Situ Cell Spreading.** Due to their intrinsic fluorescence, GSP NIH3T3 fibroblasts stably transfected with a plasmid vector (pIRESpuro3) carrying a gene for EGFP-Actin were used for in situ spreading experiments.

Cells were split at 100% previous confluency. A 4 mL aliquot of cell suspension with 35000 cells (i.e., 30 cells/mm<sup>2</sup>) was carefully placed on each sample. A dripping machine (Perfusor segura FT, b braun) supplied the dish with 0.4 mL/h deionized water to compensate for evaporation. Time lapse live cell video-microscopy measurements were started in Leica Microsystems LAS AF-TCS SP5 software 25 min after seeding of the cells. Up to four different fields of view were chosen in order to maximize the number of cells observed. Using image stacks of 18 images accounted for the tilt of the surface, the height of the cells, and the z-drift. Data analysis of the confocal data sets was conducted as well using a MATLAB program. For detailed information see the [Supporting Information](#).

**2.9. Hydrogen Evolution Measurements.** To measure hydrogen evolution, samples (cp Mg, NaOH-passivated Mg, and AV-, CDI-, and SA-coated Mg) were placed in DMEM (Biochrom) at 37 °C for 24 h. Evolved hydrogen was collected with a glass buret. Hydrogen volume was recorded after 1, 3, and 24 h and normalized to a surface area of 1 cm<sup>2</sup>.

**2.10. Electrochemical Impedance Spectroscopy.** All measurements were conducted with an electrochemical workstation “IM6”, a potentiostat “XPot”, and the corresponding “Thales” software (Zahner-Elektrik GmbH & Co. KG, Kronach, Germany). The experiments were carried out in an electrochemical cell with a three electrode setup, in which Mg samples acted as the working electrodes. A platinum sheet was used as a counter electrode, and a Ag/AgCl electrode with 3 M KCl was used as a reference electrode. DMEM (Biochrom AG) at 37 °C was used as the electrolyte. The open circuit potential (OCP) was recorded for 15 min to guarantee a stable potential for the electrochemical impedance spectroscopy (EIS) measurements (not shown). Afterward, the impedance was measured at the particular OCP of the samples in the range of 100 kHz down to 100 mHz with an excitation amplitude of  $\pm 10$  mV.

### 3. RESULTS AND DISCUSSION

**3.1. Hydrogen Evolution Measurements.** Hydrogen evolution vs immersion time (Figure 1a) shows for all samples a strong increase within the first hour, with cp Mg and CDI-coated samples showing the largest and SA-coated samples showing the lowest gas evolution (Figure 1b).

The corrosion-protective effect of AV and SA during the first hour of immersion is in agreement with previously reported data.<sup>12</sup> Similarly, the corrosion-enhancing effect of a CDI

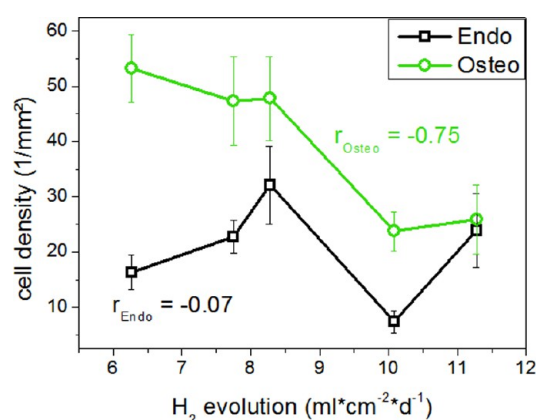


**Figure 3.** Correlation between hydrogen evolution rate  $R_{H_2}$  and cell density for cultivation of endothelial and osteosarcoma cells on differently treated Mg samples with calculated correlation coefficient  $r$ .

coating is in agreement with a corrosion attack of the sample surface during the coating procedure.<sup>12</sup>

H<sub>2</sub> evolution rates between 5 and 12 mL·cm<sup>-2</sup>·day<sup>-1</sup> during the first hour after immersion that were measured for the different samples greatly exceeded the critical value of 0.01 mL·cm<sup>-2</sup>·day<sup>-1</sup> that is regarded as biocompatible.<sup>6</sup> After 1 h, however, the rate of H<sub>2</sub> production slows for all samples, although less so in NaOH-passivated and SA-coated samples (Figure 1b). For pure Mg and AV-coated samples, gas evolution rates between 3 and 24 h after immersion approach tolerable values of around 0.02 mL·cm<sup>-2</sup>·day<sup>-1</sup>.<sup>6</sup> The significant decrease of hydrogen evolution after 3 h for all samples is attributable to a corrosion-protective layer that forms in DMEM, as has been described previously.<sup>9,22</sup> This layer formation, however, seems to be disturbed by SA coating and after NaOH passivation.

**3.2. Cell Adhesion.** Cell adhesion tests were conducted on cp Mg, NaOH-passivated Mg, and linker-coated Mg for 1 day. A prepassivation in DMEM + 20% FCS + 1% PSG for 3 days was also tested. As a reference, tissue culture plastic (TCP) was used. We measured the density and average spreading area of endothelial cells (DH1+/+) and osteosarcoma cells (MG63) after 1 day of cultivation (Figure 2). For each pretreatment and coating, two samples were prepared, and on each sample five different fields-of-view were analyzed.

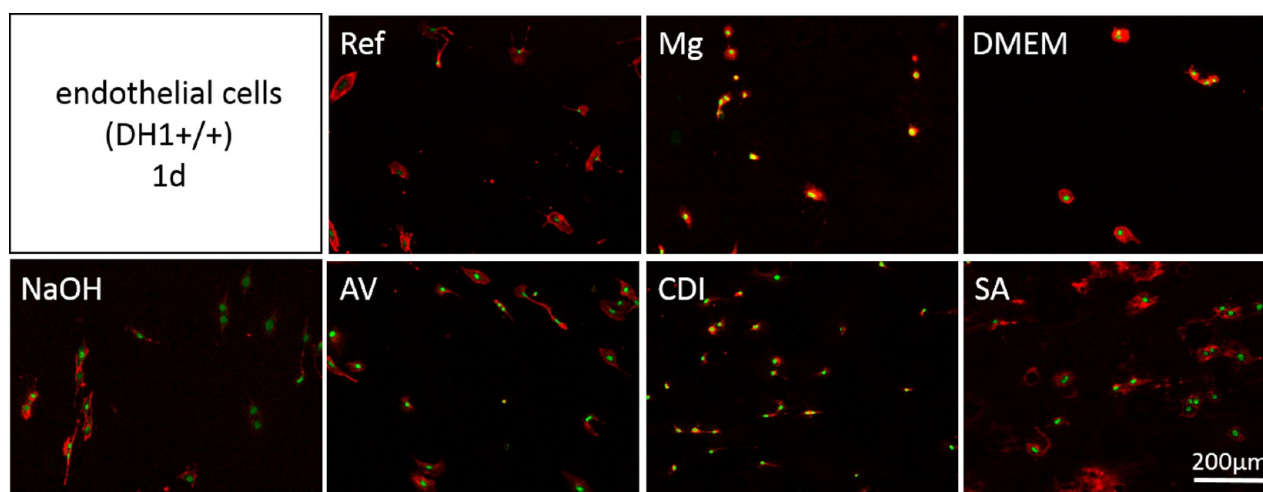


**Figure 4.** Representative images after 1 day cultivation of endothelial cells on cp Mg, after passivation in DMEM and NaOH, and after coating with AV, CDI, or SA. Cells were stained with Sytox green (nucleus) and Phalloidin red (actin cytoskeleton).

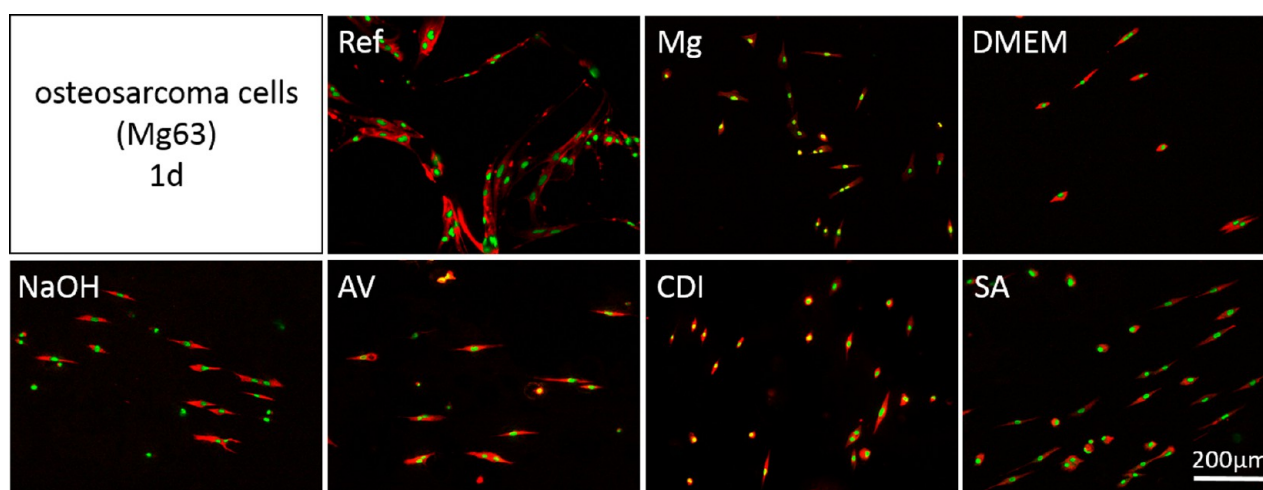


**Figure 5.** Representative images after 1 day cultivation of osteosarcoma cells on cp Mg, after passivation in DMEM and NaOH and after coating with AV, CDI, or SA. Cells were stained with Sytox green (nucleus) and Phalloidin red (cytoskeleton).

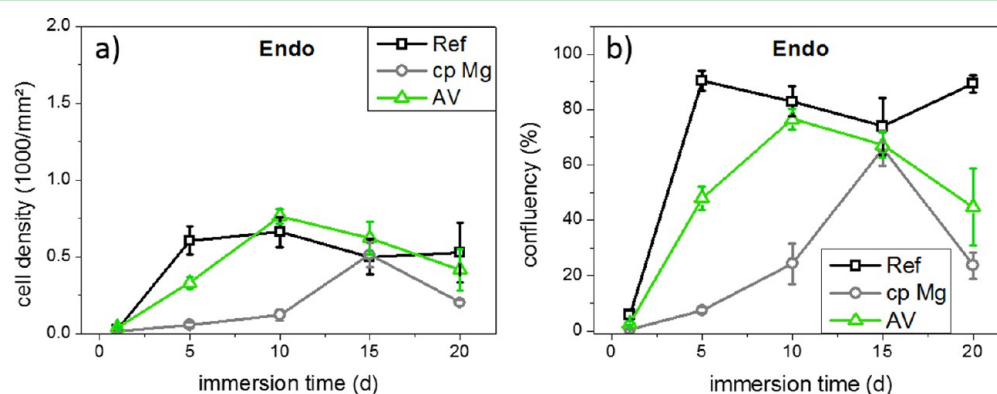


**Figure 6.** Results of long-term cell experiments with endothelial cells (DH1+/+) cultivated on cp Mg and AV-treated cp Mg. As reference, tissue culture plastic was used: (a) cell density vs time (mean  $\pm$  se,  $n = 10$ ); (b) confluency vs time (mean  $\pm$  se,  $n = 10$ ).

In general, both cell lines are able to adhere and spread on all investigated Mg samples after 1 day of cultivation. However, large differences between both cell lines are observed for adhesion and spreading on tissue culture plastic (reference), where cell density is significantly higher for osteosarcoma cells, while endothelial cells show significantly higher cell spreading

areas. Cell density also varied between differently pretreated Mg substrates, whereas cell spreading was similar on all investigated Mg samples.

For osteosarcoma cells, a slightly negative correlation ( $r = -0.75$ ) between hydrogen evolution during the first hour of immersion ( $R_{H1}$ ) and cell density was found (Figure 3),

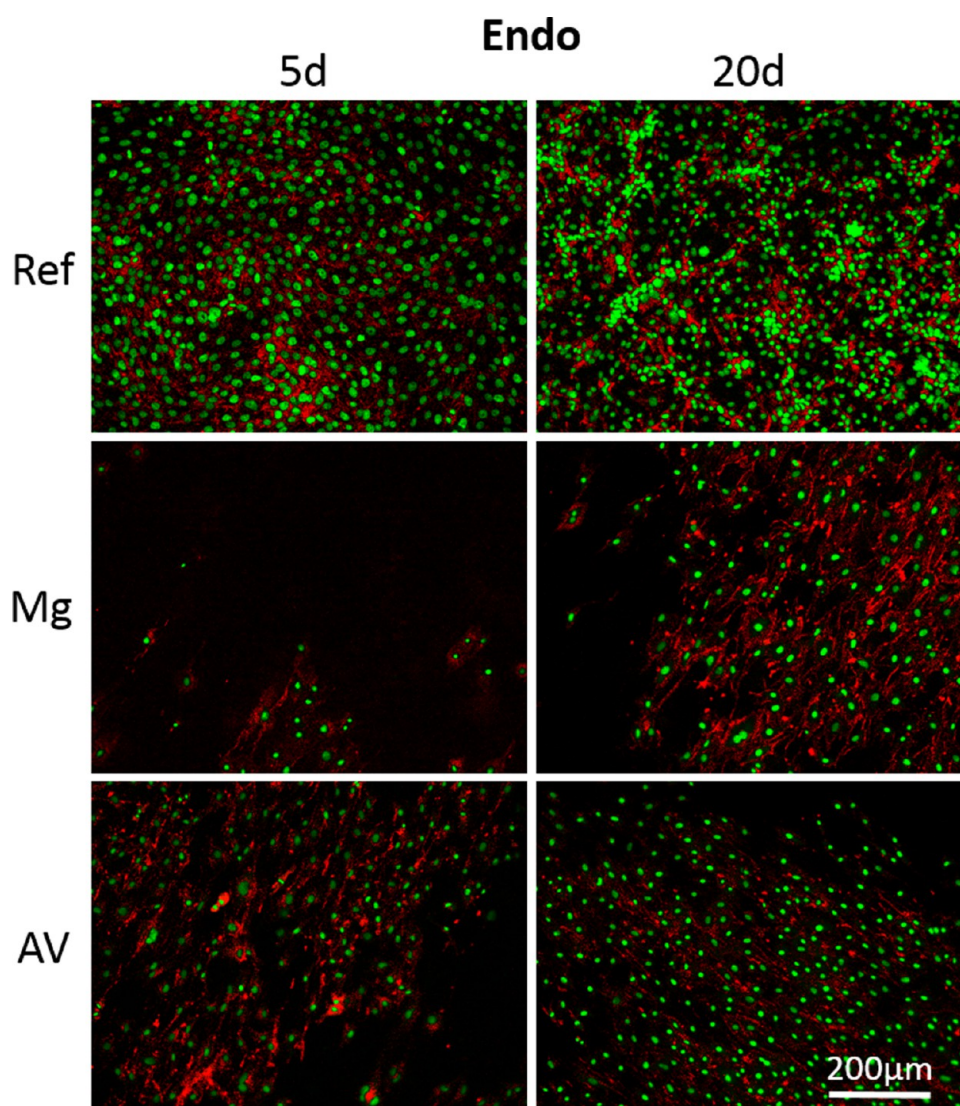


**Figure 7.** Representative images after 5 and 20 days of cultivation with endothelial cells on the tissue culture plastic, cp Mg and AV-coated Mg. Cells were stained with Sytox green (nucleus) and Phalloidin red (actin cytoskeleton).

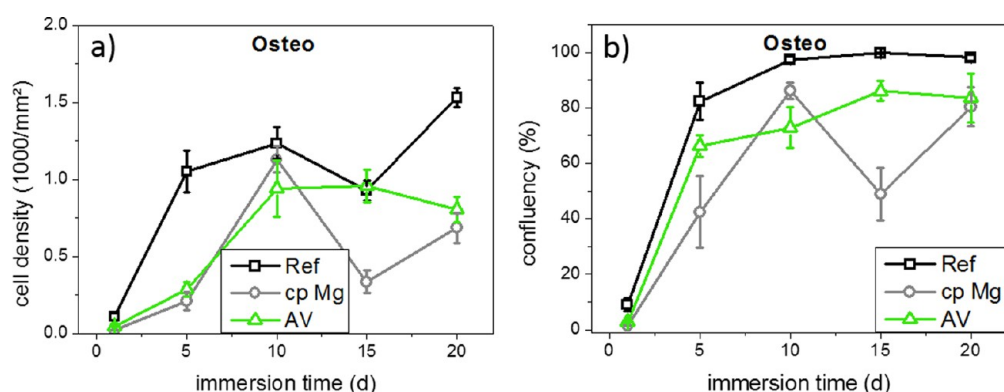


**Figure 8.** Results of the long-term cell experiments with osteosarcoma cells (MG63) cultivated on cp Mg and AV-treated cp Mg. Tissue culture plastic was used as reference: (a) cell density vs time (mean  $\pm$  se,  $n = 10$ ); (b) confluency vs time (mean  $\pm$  se,  $n = 10$ ).

indicating that cell adhesion is strongly impaired on surfaces with higher hydrogen evolution. By contrast, endothelial cells show no correlation between  $R_{\text{H}_2}$  and cell density ( $r = -0.07$ ), indicating that they can adhere better to a corroding magnesium surface. Mg corrosion is not only connected with

hydrogen evolution but also with Mg ion release as well as pH increase due to the formation of  $\text{OH}^-$  ions. However, as was shown by previous work of our group, neither the release of Mg ions nor a slight pH increase affects cell adhesion.<sup>9,23</sup> In general no strong pH increase is expected for Mg in DMEM in the

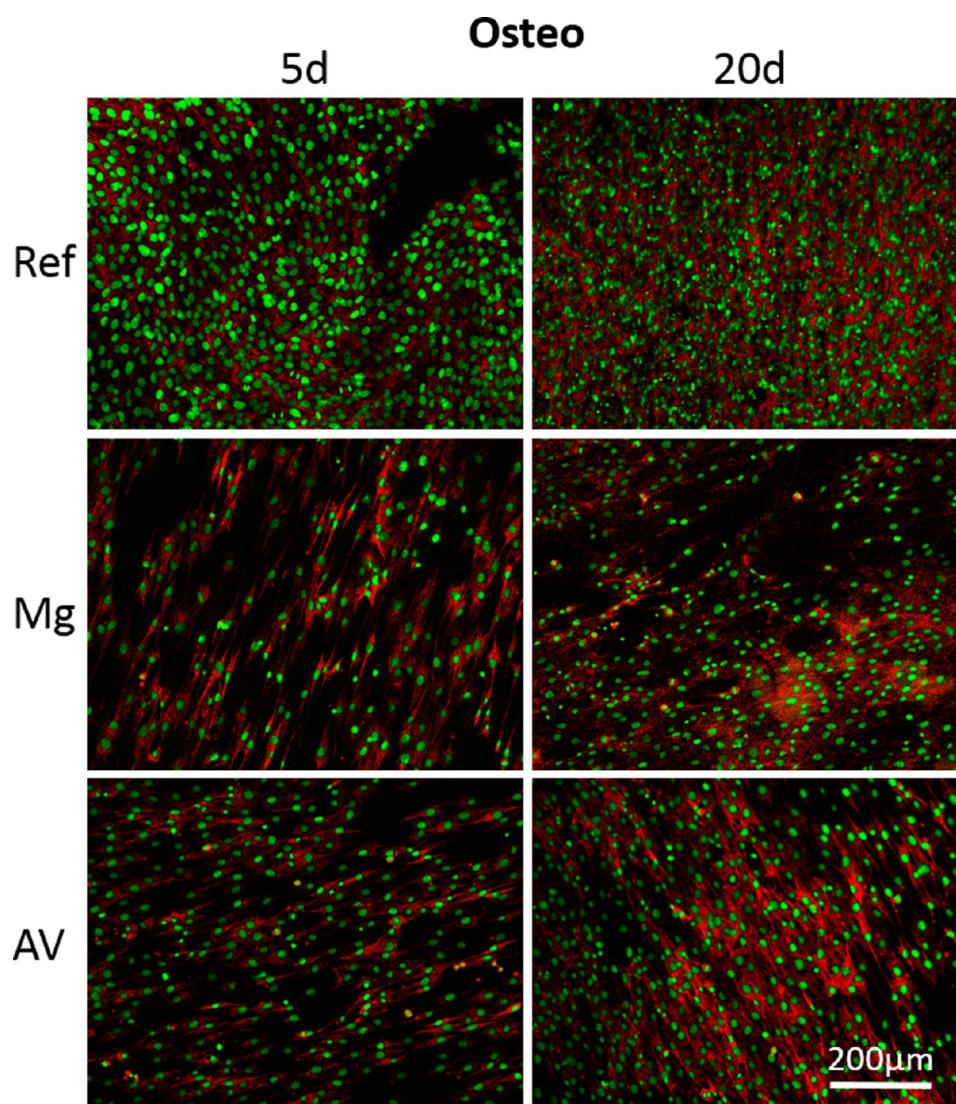


**Figure 9.** Representative images after 5 and 20 days of cultivation with osteosarcoma cells on tissue culture plastic, cp Mg and AV-coated magnesium. Cells were stained with Sytox green (nucleus) and Phalloidin red (actin cytoskeleton).

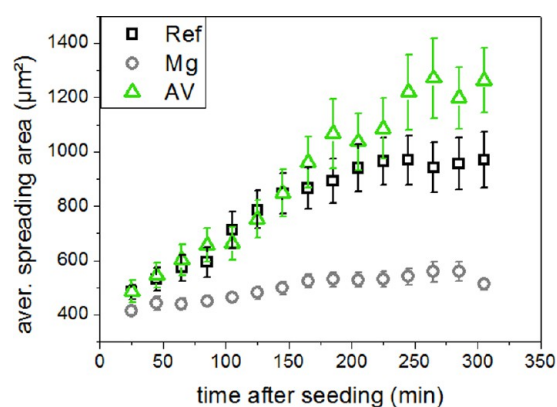


**Figure 10.** Cell spreading area (mean  $\pm$  se; TCP ref,  $n = 28$  cells; cp Mg,  $n = 38$  cells; AV,  $n = 41$  cells) vs time of fluorescent fibroblasts on cp Mg, AV-coated Mg, or tissue culture plastic as a reference.

incubator due to the strong buffering in the incubator. pH was measured during immersion of Mg in cell culture medium (DMEM + PSG + FCS) in the incubator over a period of 5 days (see the [Supporting Information](#)), showing only a minor

rise below a pH value of 8 during the first day of immersion. As a consequence, the main influencing factor affecting cell adhesion in the present case is supposed to be hydrogen evolution.

Surface morphology can as well affect cell attachment. In a previous work the different pretreatments were investigated concerning surface roughness and hydrophobicity.<sup>12</sup> Neither for endothelial nor for osteosarcoma cells could a correlation be found between surface roughness or hydrophobicity and cell adhesion.

Figures 4 and 5 show representative images after staining with Sytox green and Phalloidin red for all investigated samples cultivated with endothelial and osteosarcoma cells. Especially for osteosarcoma cells, a regular alignment of the cells with a common orientation of the major axis can be observed for all Mg but not the TCP samples. This cell alignment is attributable to the preparation of Mg samples: As samples are ground, visible grinding grooves appear on the surface that cause the cells to align.<sup>24,25</sup>

**3.3. Cell Growth.** After cell adhesion tests for 1 day, long-term experiments with mouse endothelial cells (DH1+/+) were

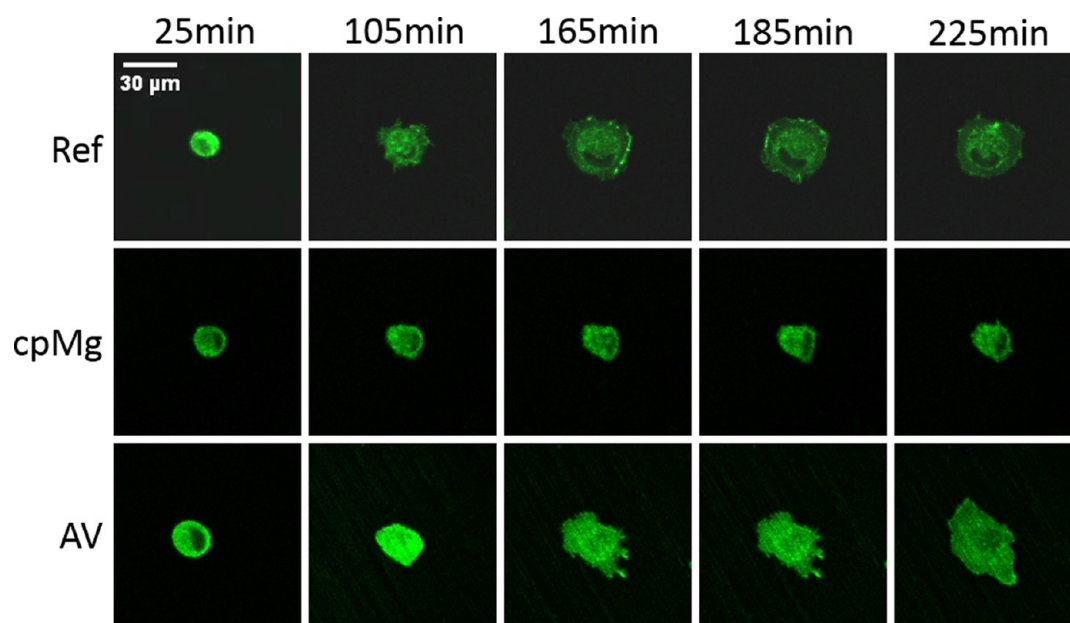


**Figure 11.** Representative images of fluorescently labeled fibroblasts after 25, 105, 165, 185, and 225 min of cell cultivation on the tissue culture plastic, cp Mg, and Av-coated Mg.

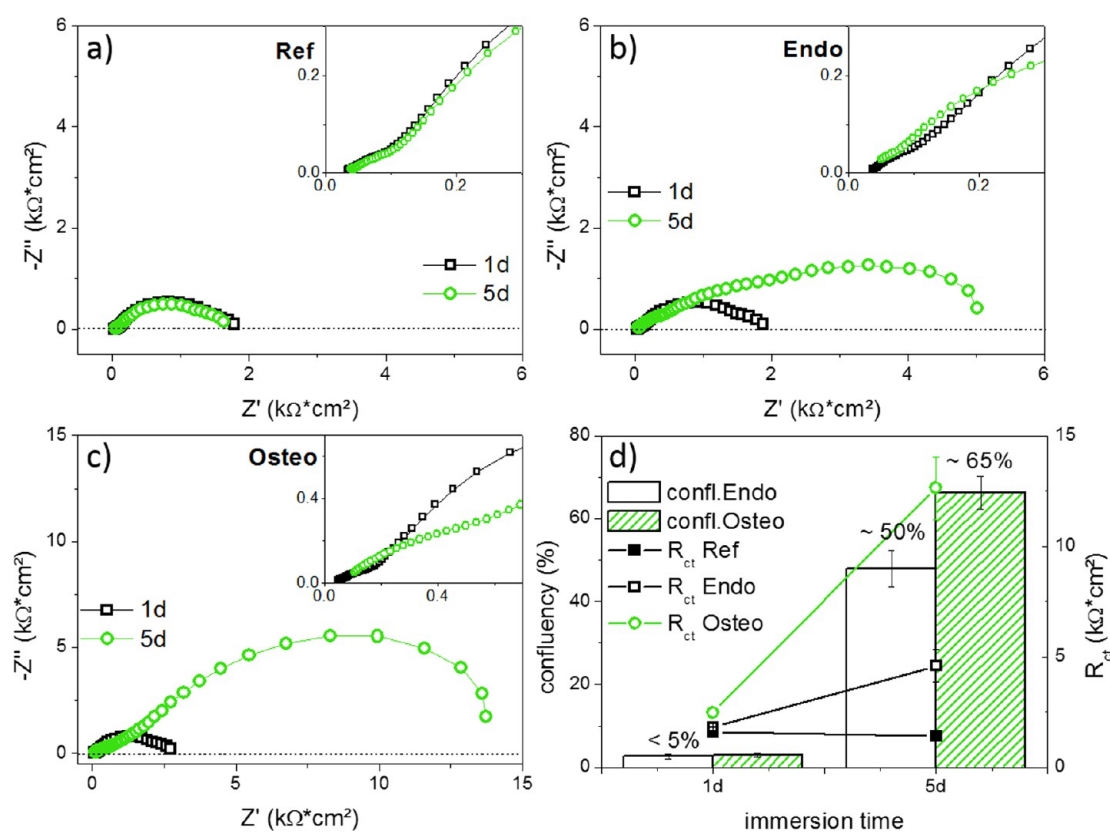


**Figure 12.** EIS after 1 and 5 days: (a) Nyquist plots of AV-coated Mg samples without cells immersed in cell culture medium; (b) samples incubated with endothelial cells (DH1+/+); (c) samples incubated with osteosarcoma cells (Mg63); (d) comparison of calculated total charge transfer resistances vs time.

conducted for up to 20 days on cp Mg, AV-coated Mg, and tissue culture plastic as reference (Figure 6).

On tissue culture plastic, cell density and confluency reach a maximum after 5 days (cell density  $\sim 600$  cells/mm<sup>2</sup>; confluency  $\sim 90\%$ ) and remain similarly high over longer time periods. On cp Mg, cell density and confluency show a

much slower increase and reach a maximum after 15 days (cell density  $\sim 500$  cells/mm<sup>2</sup>; confluency  $\sim 65\%$ ). Between day 15 and day 20, a dramatic decrease for both values is observed as large patches of the endothelial cell layer detaches from the substrate (Figure 7). Nonetheless, these results demonstrate that long-term cell growth of endothelial cells on cp Mg is

possible. Coating of Mg samples with AV enhance cell growth so that cell density and confluency reach a maximum after 10 days with values similar to those achieved on tissue cultured plastic (cell density  $\sim 600$  cells/mm<sup>2</sup>; confluency  $\sim 80\%$ ). After 10 days of culture, cell density and confluency start to decline as patches of the endothelial cell layer detach from the substrate, but this decline is less dramatic than on cp Mg. These results demonstrate that coating with AV increases the biocompatibility of Mg.

Long-term cell experiments with osteosarcoma cells (MG63) on these three substrates (Figure 8) give qualitatively similar results, but cell density and confluency are higher on all substrates compared to endothelial cells, and the differences between the substrates are less pronounced. Even on cp Mg, cells show high density (600 cells/mm<sup>2</sup>) and confluency (80%) after 20 days of culture, indicating that the higher substrate adhesiveness after AV coating is not a prerequisite for the long-term growth of osteosarcoma cells. Some representative images after cell staining are shown in Figure 9 in order to convey a visual impression of long-term cell experiments with osteosarcoma cells.

**3.4. Cell Spreading.** To study the influence of the coating on the initial cell spreading behavior, fluorescent fibroblasts were seeded onto pure or AV-coated magnesium samples, or onto tissue culture plastic as a reference, and the cell spreading area was measured in situ between 25 and 300 min after seeding, using a confocal microscope equipped with a water dipping objective (Figure 10 and Figure 11).

The spreading area of fibroblasts at the start of the experiment (25 min after seeding) is similar on all samples ( $\sim 400$ – $500$   $\mu\text{m}^2$ ), which is only slightly larger than the projected area of round, nonadherent cells. The spreading area of cells plated on TCP as reference increases steadily for 200 min and reaches values of  $1000$   $\mu\text{m}^2$ . The spreading behavior of cells on AV-coated Mg is similar, but the spreading area continues to increase after 200 min and reaches values around  $1200$   $\mu\text{m}^2$ , indicating that the substrate is even more adhesive than tissue culture plastic. By contrast, cells seeded on cp Mg show only a minor increase of the spreading area to about  $500$   $\mu\text{m}^2$  over a time course of 5 h, indicating limited adhesiveness of the substrate.

**3.5. Influence of Cell Adhesion and Proliferation on Corrosion Behavior.** To investigate the influence of an endothelial (DH1+/+) or osteosarcoma (MG63) cell layer on the corrosion behavior of AV-coated magnesium samples, electrochemical impedance spectra (EIS) were measured in DMEM at 37 °C after 1 and 5 days of culture. As reference, EIS was measured from AV-coated but cell-free Mg samples immersed for 1 and 5 days in cell culture medium (DMEM + 20% FCS + 1% PSG).

In general, the Nyquist plots of all investigated samples (Figure 12a–c) show similar shapes, indicating similar corrosion mechanisms. A major influence of cell layers on the surface is seen in increasing the charge transfer resistance (which is inversely related to the corrosion rate). To analyze the EIS results, the total charge transfer resistances,  $R_{ct}$  (value at lowest frequency minus value at highest frequency), were calculated and compared (Figure 12d). After 1 day of culture,  $R_{ct}$  values of samples with or without cells are similar, indicating no significant influence of cell attachment on the corrosion behavior. However, the results of the one-day-cell-experiments show surface coverage of less than 5% for both cell lines (Figure 12d), and the influence after 1 day cultivation can be estimated

as minor. By contrast, after 5 days of culture, large differences between the samples emerge, whereby the cell-incubated samples show larger charge transfer resistances compared to the cell-free samples. The differences between endothelial and osteosarcoma cells are at least partially attributable to the different degrees of confluency, which reached a surface coverage for DH1+/+ cells of about 40–50% after 5 days, compared to 60–70% for MG63 cells. These results indicate that surface coverage with cells increases the corrosion resistance of magnesium in culture medium.

## 4. CONCLUSION

Our data show that long-term adhesion, spreading, and growth of cells on untreated magnesium is possible. However, passivation and coating of the Mg surface with SA, CDI, and particularly AV markedly reduced initial hydrogen evolution and enhanced biocompatibility (cell adhesion, spreading, and growth) compared to bare magnesium. A positive effect of cell adhesion on corrosion resistance could be found.

## ■ ASSOCIATED CONTENT

### Supporting Information

The Supporting Information is available free of charge on the ACS Publications website at DOI: 10.1021/acsami.6b01747.

Data analysis of in situ cell spreading (PDF)

## ■ AUTHOR INFORMATION

### Corresponding Author

\*E-mail: sannkaisa.virtanen@fau.de.

### Author Contributions

<sup>§</sup>V.W., A.S., B.F., and S.V. contributed equally to this work.

### Notes

The authors declare no competing financial interest.

## ■ ACKNOWLEDGMENTS

The authors thank DFG for funding (DFG Grant VI 350/7-1, for all authors).

## ■ ABBREVIATIONS

AV, aminopropyltriethoxysilane plus vitamin C  
CDI, carbonyldiimidazole  
DH1+/+, murine endothelial cell type  
DMEM, Dulbecco's modified Eagle's medium  
(D)PBS, (Dulbecco's) phosphate-buffered saline  
EIS, electrochemical impedance spectroscopy  
FCS, fetal calf serum  
GSP NIH/3T3, fluorescently labeled fibroblasts  
MG63, human osteosarcoma cell type  
SA, stearic acid  
TCP, tissue culture plastic

## ■ REFERENCES

- (1) Hornberger, H.; Virtanen, S.; Boccacini, A. R. Biomedical Coatings on Magnesium Alloys – A Review. *Acta Biomater.* **2012**, *8* (7), 2442–2455.
- (2) Witte, F.; Hort, N.; Vogt, C.; Cohen, S.; Kainer, K. U.; Willumeit, R.; Feyerabend, F. Degradable Biomaterials Based on Magnesium Corrosion. *Curr. Opin. Solid State Mater. Sci.* **2008**, *12* (5–6), 63–72.
- (3) Geis-Gerstorfer, J.; Schille, C.; Schweizer, E.; Rupp, F.; Scheideler, L.; Reichel, H. P.; Hort, N.; Nolte, A.; Wendel, H. P. Blood Triggered Corrosion of Magnesium Alloys. *Mater. Sci. Eng., B* **2011**, *176* (20), 1761–1766.

- (4) Lévesque, J.; Hermawan, H.; Dubé, D.; Mantovani, D. Design of a Pseudo-Physiological Test Bench Specific to the Development of Biodegradable Metallic Biomaterials. *Acta Biomater.* **2008**, *4* (2), 284–295.
- (5) Witte, F.; Fischer, J.; Nellesen, J.; Crostack, H. A.; Kaese, V.; Pisch, A.; Beckmann, F.; Windhagen, H. In Vitro and In Vivo Corrosion Measurements of Magnesium Alloys. *Biomaterials* **2006**, *27* (7), 1013–1018.
- (6) Song, G. L. Control of Biodegradation of Biocompatible Magnesium Alloys. *Corros. Sci.* **2007**, *49* (4), 1696–1701.
- (7) Song, G. L. Recent Progress in Corrosion and Protection of Magnesium Alloys. *Adv. Eng. Mater.* **2005**, *7* (7), 563–586.
- (8) Zeng, R.; Dietzel, W.; Witte, F.; Hort, N.; Blawert, C. Progress and Challenge for Magnesium Alloys as Biomaterials. *Adv. Eng. Mater.* **2008**, *10* (8), B3–B14.
- (9) Seuss, F.; Seuss, S.; Turhan, M. C.; Fabry, B.; Virtanen, S. Corrosion of Mg Alloy AZ91D in the Presence of Living Cells. *J. Biomed. Mater. Res., Part B* **2011**, *99B* (2), 276–281.
- (10) Kasemo, B. Biological Surface Science. *Surf. Sci.* **2002**, *500* (1–3), 656–677.
- (11) Wilson, C. J.; Clegg, R. E.; Leavesley, D. I.; Percy, M. J. Mediation of Biomaterial-Cell Interactions by Adsorbed Proteins: A Review. *Tissue Eng.* **2005**, *11* (1–2), 1–18.
- (12) Wagener, V.; Killian, M. S.; Turhan, C. M.; Virtanen, S. Albumin Coating on Magnesium via Linker Molecules-Comparing Different Coating Mechanisms. *Colloids Surf., B* **2013**, *103*, 586–594.
- (13) Song, Y. Y.; Schmidt-Stein, F.; Bauer, S.; Schmuki, P. Amphiphilic TiO<sub>2</sub> Nanotube Arrays: an Actively Controllable Drug Delivery System. *J. Am. Chem. Soc.* **2009**, *131* (12), 4230–2.
- (14) Song, Y. Y.; Hildebrand, H.; Schmuki, P. Optimized Monolayer Grafting of 3-Aminopropyltriethoxysilane onto Amorphous, Anatase and Rutile TiO<sub>2</sub>. *Surf. Sci.* **2010**, *604* (3–4), 346–353.
- (15) Tiller, J.; Berlin, P.; Klemm, D. A Novel Efficient Enzyme-Immobilization Reaction on NH<sub>2</sub> Polymers by Means of L-Ascorbic Acid. *Biotechnol. Appl. Biochem.* **1999**, *30* (2), 155–162.
- (16) Bauer, S.; Park, J.; Pittrof, A.; Song, Y.-Y.; von der Mark, K.; Schmuki, P. Covalent Functionalization of TiO<sub>2</sub> Nanotube Arrays with EGF and BMP-2 for Modified Behavior Towards Mesenchymal Stem Cells. *Integr. Biol.* **2011**, *3* (9), 927–936.
- (17) Wang, Y. H.; Wang, W.; Zhong, L.; Wang, J.; Jiang, Q. L.; Guo, X. Y. Super-hydrophobic Surface on Pure Magnesium Substrate by Wet Chemical Method. *Appl. Surf. Sci.* **2010**, *256* (12), 3837–3840.
- (18) Oliveira, E. M.; Beyer, S.; Heinze, J. SECM Characterization of Immobilised Enzymes by Self-assembled Monolayers on Titanium Dioxide Surfaces. *Bioelectrochemistry* **2007**, *71* (2), 186–191.
- (19) Adden, N.; Gamble, L. J.; Castner, D. G.; Hoffmann, A.; Gross, G.; Menzel, H. Phosphonic Acid Monolayers for Binding of Bioactive Molecules to Titanium Surfaces. *Langmuir* **2006**, *22* (19), 8197–8204.
- (20) Sheller, N. B.; Petrash, S.; Foster, M. D.; Tsukruk, V. V. Atomic Force Microscopy and X-ray Reflectivity Studies of Albumin Adsorbed onto Self-Assembled Monolayers of Hexadecyltrichlorosilane. *Langmuir* **1998**, *14* (16), 4535–4544.
- (21) Tremsina, Y. S.; Sevastianov, V. I.; Petrash, S.; Dando, W.; Foster, M. D. Competitive Adsorption of Human Serum Albumin and Gamma-Globulin from a Binary Protein Mixture onto Hexadecyltrichlorosilane Coated Glass. *J. Biomater. Sci., Polym. Ed.* **1998**, *9* (2), 151–161.
- (22) Virtanen, S. Biodegradable Mg and Mg alloys: Corrosion and Biocompatibility. *Mater. Sci. Eng., B* **2011**, *176* (20), 1600–1608.
- (23) Keim, S.; Brunner, J. G.; Fabry, B.; Virtanen, S. Control of Magnesium Corrosion and Biocompatibility with Biomimetic Coatings. *J. Biomed. Mater. Res., Part B* **2011**, *96B* (1), 84–90.
- (24) Flemming, R. G.; Murphy, C. J.; Abrams, G. A.; Goodman, S. L.; Nealey, P. F. Effects of Synthetic Micro- and Nano-structured Surfaces on Cell Behavior. *Biomaterials* **1999**, *20* (6), 573–588.
- (25) Teixeira, A. I.; Abrams, G. A.; Bertics, P. J.; Murphy, C. J.; Nealey, P. F. Epithelial Contact Guidance on Well-Defined Micro- and Nanostructured Substrates. *J. Cell Sci.* **2003**, *116* (10), 1881–1892.